Article

Cell Reports

2-HG Inhibits Necroptosis by Stimulating DNMT1-Dependent Hypermethylation of the *RIP3* Promoter

Graphical Abstract

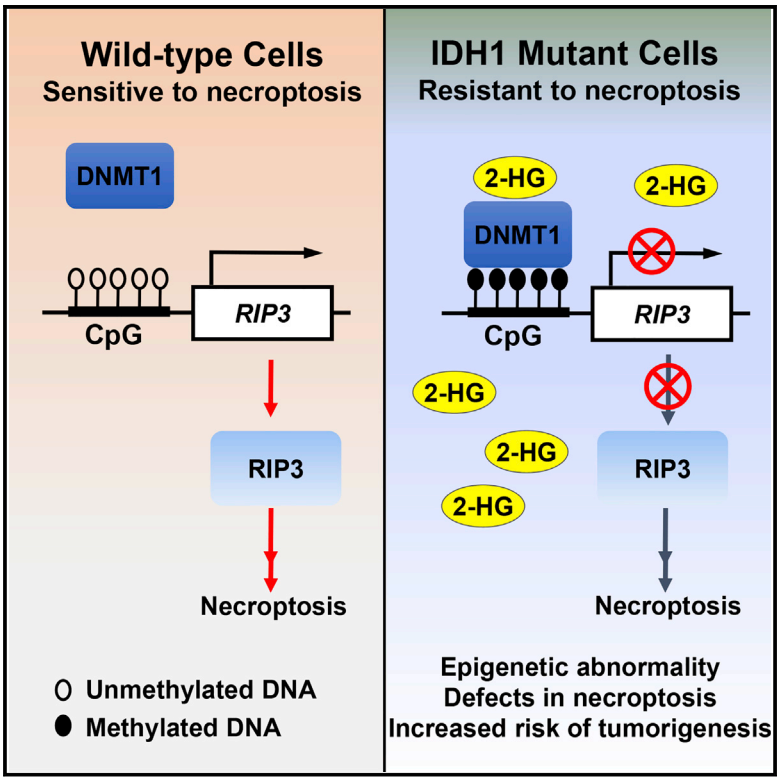

Highlights

- 2-HG profoundly reduces RIP3 protein and consequently impairs necroptosis
- 2-HG binds to DNMT1 and stimulates its association with the *RIP3* promoter
- TET2 is not involved in transcriptional silencing of RIP3 by 2-HG
- Loss of RIP3-mediated necroptosis contributes to tumorigenesis driven by 2-HG

Authors

Zhentao Yang, Bin Jiang, Yan Wang, ..., Tak Wah Mak, Qinxi Li, Jiahuai Han

Correspondence

liqinxi@xmu.edu.cn (Q.L.),
jhan@xmu.edu.cn (J.H.)

In Brief

Yang et al. report that oncometabolite 2-HG produced by tumor-associated IDH1 mutation physically binds to DNMT1 and stimulates its association with the *RIP3* promoter, inducing hypermethylation that reduces RIP3 protein and consequently impaired RIP3-dependent necroptosis. Loss of RIP3-mediated necroptosis contributes to tumorigenesis driven by 2-HG.

Yang et al., 2017, Cell Reports *19*, 1846–1857
May 30, 2017 © 2017 The Author(s).
http://dx.doi.org/10.1016/j.celrep.2017.05.012

OPEN ACCESS
CellPress

Cell Reports
Article

2-HG Inhibits Necroptosis by Stimulating DNMT1-Dependent Hypermethylation of the *RIP3* Promoter

Zhentao Yang,[1,7] Bin Jiang,[1,7] Yan Wang,[1,7] Hengxiao Ni,[1] Jia Zhang,[1] Jinmei Xia,[2] Minggang Shi,[3] Li-Man Hung,[4,5] Jingsong Ruan,[1] Tak Wah Mak,[6] Qinxi Li,[1,*] and Jiahuai Han[1,8,*]

[1]State Key Laboratory of Cellular Stress Biology, Innovation Center for Cell Signaling Network, School of Life Sciences, Xiamen University, Xiamen, Fujian 361102, China

[2]Key Laboratory of Marine Biogenetic Resources, Third Institute of Oceanography, State Oceanic Administration, Xiamen, Fujian 361102, China

[3]Department of Neurosurgery, Huanhu Hospital, No. 6 Jizhao Road, Jinnan District, Tianjin 30050, China

[4]Department of Biomedical Sciences and Graduate Institute of Biomedical Sciences, College of Medicine, Chang Gung University, Tao-Yuan, Taiwan 111, ROC

[5]Department of Anesthesiology, Chang Gung Memorial Hospital, Tao-Yuan, Taiwan 111, ROC

[6]The Campbell Family Institute for Breast Cancer Research, Ontario Cancer Institute, University Health Network, Toronto, ON M5G 2C1, Canada

[7]These authors contributed equally

[8]Lead Contact

*Correspondence: liqinxi@xmu.edu.cn (Q.L.), jhan@xmu.edu.cn (J.H.)

http://dx.doi.org/10.1016/j.celrep.2017.05.012

SUMMARY

2-hydroxyglutarate-(2-HG)-mediated inhibition of TET2 activity influences DNA hypermethylation in cells harboring mutations of isocitrate dehydrogenases 1 and 2 (IDH1/2). Here, we show that 2-HG also regulates DNA methylation mediated by DNA methyltransferase 1 (DNMT1). DNMT1-dependent hypermethylation of the *RIP3* promoter occurred in both IDH1 R132Q knockin mutant mouse embryonic fibroblast (MEFs) and 2-HG-treated wild-type (WT) MEFs. We found that 2-HG bound to DNMT1 and stimulated its association with the *RIP3* promoter, inducing hypermethylation that reduces RIP3 protein and consequently impaired RIP3-dependent necroptosis. In human glioma samples, RIP3 protein levels correlated negatively with IDH1 R132H levels. Furthermore, ectopic expression of RIP3 in transformed IDH1-mutated MEFs inhibited the growth of tumors derived from these cells following transplantation into nude mice. Thus, our research sheds light on a mechanism of 2-HG-induced DNA hypermethylation and suggests that impaired necroptosis contributes to the tumorigenesis driven by IDH1/2 mutations.

INTRODUCTION

DNA methylation is an epigenetic mechanism used by cells to control gene expression. Such methylation occurs mainly on a gene's CpG islands, and the extent of this methylation is determined by the balance between methylation and demethylation processes. In mammalian cells, DNA methylation is carried out by three DNA methyltransferases (DNMTs): DNMT1; DNMT3a; and DNMT3b. DNMT1 is the most abundant DNMT in mammalian cells and responsible for routine methylation maintenance throughout the life of an organism, whereas DNMT3a and DNMT3b are de novo DNMTs that act to set up DNA methylation patterns early in development (Bird and Wolffe, 1999; Li, 2002; Reik et al., 2001). DNA demethylation occurs mainly at 5-methylcytosine (5mC) residues and is initialized by the ten-eleven translocation (TET) proteins: TET1; TET2; and TET3. The TETs act as dioxygenases to convert 5mC to 5-hydroxymethylcytosine (5hmC), a step crucial for the subsequent removal of the methyl group from the cytosine (He et al., 2011b; Ito et al., 2010, 2011; Tahiliani et al., 2009).

Isocitrate dehydrogenase 1 (IDH1) normally converts isocitrate to α-ketoglutarate (α-KG) (Haselbeck and McAlister-Henn, 1993). Mutations (R132H/Q/C/S/L/G/V/P) of this enzyme are frequent in glioma, acute myeloid leukemia (AML), chondrosarcoma, cholangiocarcinoma, paraganglioma, colon cancer, prostate cancer, and lung cancer (Abbas et al., 2010; Amary et al., 2011; Bleeker et al., 2009; Borger et al., 2012; De Carli et al., 2009; Ducray et al., 2009; Gaal et al., 2010; Kang et al., 2009; Mardis et al., 2009; Pansuriya et al., 2011; Parsons et al., 2008; Sequist et al., 2011; Sjöblom et al., 2006). Interestingly, these mutations confer upon IDH1 an abnormal activity that converts α-KG to 2-hydroxyglutarate (2-HG) (Dang et al., 2009; Figueroa et al., 2010; Ward et al., 2010). In glioma samples harboring mutated IDH, 2-HG accumulates up to 35 μmol/g, a concentration ~100-fold greater than that in control samples (Dang et al., 2009). Due to the structural similarity between 2-HG and α-KG, 2-HG has been thought to competitively inhibit α-KG-dependent

This is an open access article under the CC BY-NC-ND license (http://creativecommons.org/licenses/by-nc-nd/4.0/).

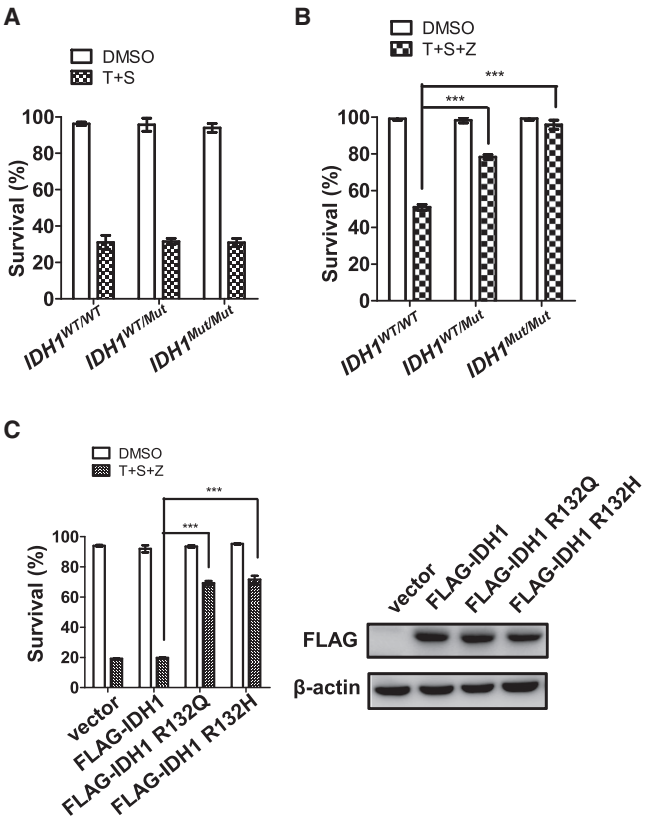

Figure 1. IDH1 R132 Mutations Desensitize MEFs to TNF-α-Induced Necroptosis

(A) Survival of *IDH1*$^{WT/WT}$, *IDH1*$^{WT/Mut}$, and *IDH1*$^{Mut/Mut}$ MEFs that were treated with DMSO (vehicle) or TNF-α (T) (30 ng/mL) + Smac mimetic (S) (1 μM) for 24 hr followed by flow cytometric viability analysis. Unless otherwise indicated, all quantitative data are presented as the mean ± SD of triplicate samples. All results are representative of three independent experiments. *$p < 0.05$; **$p < 0.01$; ***$p < 0.001$ by unpaired Student's t test.

(B) Survival of *IDH1*$^{WT/WT}$, *IDH1*$^{WT/Mut}$, and *IDH1*$^{Mut/Mut}$ MEFs that were treated with DMSO or TNF-α (30 ng/mL) + Smac mimetic (1 μM) + zVAD (Z) (20 μM) for 14 hr followed by viability analysis as in (A).

(C) Left: survival of WT MEFs that were infected with empty lentivirus (vector) or lentivirus expressing FLAG-tagged WT IDH1, IDH1-R132Q, or IDH1-R132H, as indicated. At 96 hr post-infection, cells were treated for 20 hr with DMSO or T + S + Z as in (B) and analyzed for viability. Right: western blot to detect the indicated proteins in lysates of the cells in the left panel is shown. β-actin, loading control.

dioxygenases, such as TET2 and histone demethylases (Figueroa et al., 2010; Losman et al., 2013; Xu et al., 2011), resulting in DNA and histone hypermethylation in cells bearing IDH1 mutations. In addition, 2-HG blocks prolyl hydroxylase and thereby stabilizes hypoxia-inducible factor-1α (HIF-1α), inducing transcriptional activation of HIF-1α-dependent genes. These alterations to gene expression mediated by mutated IDH1 disrupt cell differentiation and promote tumor cell initiation, growth, invasion, and angiogenesis (Noushmehr et al., 2010; Sasaki et al., 2012b; Turcan et al., 2012; Xu et al., 2011; Zhao et al., 2009). However, our knowledge of precisely which genes are regulated by 2-HG-induced DNA methylation and the biological functions of such regulation is limited.

Necroptosis is a form of programmed death in which cells die with a necrotic phenotype. Tumor necrosis factor-α (TNF-α)-induced necroptosis is the prototypic model system, and its intensive study has revealed crucial mechanistic details. Receptor interacting protein 1 (RIP1) receives death signals from the TNF-α receptor complex and recruits RIP3 to form the necrosome. Within the necrosome, RIP3 undergoes auto-phosphorylation and recruits and phosphorylates mixed lineage kinase domain-like (MLKL) protein. Phosphorylated MLKL then translocates to the plasma membrane to execute necroptosis (Chen et al., 2016). Among these players, RIP3 is the most important determinant of necroptosis: whereas RIP1 can direct death signals toward either apoptosis or necroptosis, RIP3 dictates that death signals passed on by RIP1 lead solely to necroptosis (Zhang et al., 2009). Significantly, RIP3 expression is often silenced in cancer cells due to DNMT1-dependent methylation of the *RIP3* gene near its transcriptional start site (TSS) (Koo et al., 2015). These data suggest that, like apoptosis, necroptosis of incipient cancer cells is a barrier to tumorigenesis.

In this study, we report that IDH1 mutations inhibit TNF-α-induced necroptosis in wild-type (WT) mouse embryonic fibroblasts (MEFs) and other cell types. This inhibition results from downregulation of RIP3 expression caused by 2-HG, the product of mutated IDH1. 2-HG induces DNA hypermethylation of the *RIP3* promoter near its TSS by binding to DNMT1 and stimulating its association with the *RIP3* promoter. This downregulation of RIP3 associated with IDH1 mutation also occurs in humans because RIP3 levels in human oligodendroglioma samples correlate negatively with levels of IDH1 R132H protein. Furthermore, ectopic RIP3 expression in transformed IDH1 R132Q MEFs limited their ability to drive tumor growth in recipient mice. Thus, 2-HG's effects on DNMT1 and RIP3 that result in resistance to necroptosis represent part of the contribution of IDH1 mutations to tumorigenesis.

RESULTS

IDH1 R132 Mutations Desensitize MEFs to TNF-α-Induced Necroptosis

To expand our studies of the cellular consequences of IDH1 R132 mutations, we evaluated the effects of the IDH1 R132Q mutation on TNF-α-induced cell death. MEFs were isolated from the embryos of IDH1 R132Q knockin mice (Inoue et al., 2016; Sasaki et al., 2012a, 2012b). The lox-stop-lox (LSL) cassette in these cells was excised with Cre recombinase to generate immortalized MEF lines of three different genotypes: *IDH1*$^{WT/WT}$; *IDH1*$^{WT/Mut}$ (where Mut = R132Q); and *IDH1*$^{Mut/Mut}$. It is known that TNF-α induces the apoptosis of MEFs in the presence of the inhibitor of apoptosis proteins (IAPs) antagonist Smac mimetic but triggers necroptosis in the presence of Smac mimetic plus the pan-caspase inhibitor zVAD (Wang et al., 2008; Zhang et al., 2011). We found that *IDH1*$^{WT/Mut}$ and *IDH1*$^{Mut/Mut}$ MEFs were just as sensitive to TNF-α-induced apoptosis as *IDH1*$^{WT/WT}$ MEFs (Figure 1A) but that *IDH1*$^{WT/Mut}$ and *IDH1*$^{Mut/Mut}$ MEFs were less sensitive to TNF-α-induced necroptosis than *IDH1*$^{WT/WT}$ MEFs (Figure 1B). To confirm that this decreased sensitivity to TNF-α-induced necroptosis was

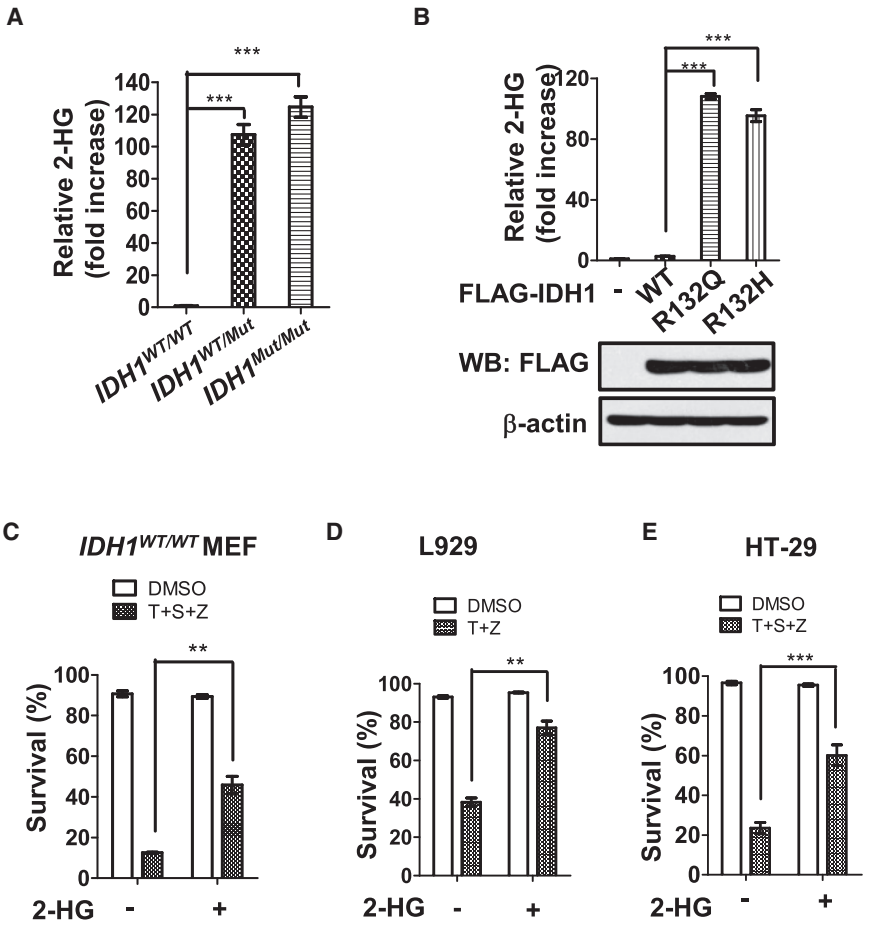

Figure 2. 2-HG Inhibits TNF-α-Induced Necroptosis

(A) LC-MS determination of 2-HG production by MEFs of the indicated genotypes. Results are the mean fold increase in 2-HG level relative to that in $IDH1^{WT/WT}$ MEFs.

(B) Top: LC-MS determination of 2-HG production by HEK293T cells that were transfected with equal amounts of plasmids expressing IDH1 R132Q or IDH1 R132H, as indicated. Data are expressed as in (A). Bottom: western blot to detect Flag-tagged proteins in the cells in the top panel is shown. The fold increase in 2-HG relative to that in cells expressing vector control was normalized to protein levels.

(C–E) Survival of $IDH1^{WT/WT}$ MEFs (C), L929 cells (D), and HT-29 cells (E) that were left untreated (−) or pretreated (+) with 2-HG (2 mM) for 7 days followed by treatment with the indicated stimuli (T + Z or T + S + Z) for 20 hr (C), 4 hr (D), or 24 hr (E). Cell viability was determined as in Figure 1.

due to IDH1 mutation, we separately overexpressed WT, R132Q, or R132H mutant IDH proteins in WT MEFs to determine their effects on TNF-α-induced necroptosis. Overexpression of IDH1 R132Q or R132H, but not WT IDH1, inhibited TNF-α-induced necroptosis (Figure 1C). Thus, expression of IDH1 mutant proteins in MEF desensitizes these cells to TNF-α-induced necroptosis.

2-HG Inhibits TNF-α-Induced Necroptosis

A prominent feature associated with IDH1 R132 mutation is the synthesis of extremely high levels of the abnormal product 2-HG (Dang et al., 2009; Figueroa et al., 2010; Ward et al., 2010). We explored whether the desensitization to TNF-α-induced necroptosis we observed in our mutant MEFs was caused by their excessive 2-HG production. First, we employed liquid chromatography spectrometry (LC-MS) to determine 2-HG concentrations and detected much higher 2-HG levels in $IDH1^{WT/Mut}$ and $IDH1^{Mut/Mut}$ MEFs than in $IDH1^{WT/WT}$ MEFs (Figure 2A). Ectopic expression of IDH1 R132Q or IDH1 R132H in HEK293T cells also resulted in elevated intracellular 2-HG (Figure 2B). We then examined whether treatment of MEFs with exogenous 2-HG could induce resistance to TNF-α-induced necroptosis. Indeed, pretreatment of $IDH1^{WT/WT}$ MEFs with cell-permeable octyl-2-HG attenuated TNF-α-induced necroptosis (Figure 2C). Similar results were obtained using the mouse L929 and human HT-29 cell lines (Figures 2D and 2E). These data demonstrate that 2-HG inhibits TNF-α-induced necroptosis in a broad range of mammalian cell types.

2-HG Desensitizes Cells to TNF-α-Induced Necroptosis by Suppressing RIP3 Expression

Because RIP3, RIP1, and MLKL are all key components of the necroptosis pathway, we determined the levels of these three proteins in $IDH1^{WT/WT}$, $IDH1^{WT/Mut}$, and $IDH1^{Mut/Mut}$ MEFs. Interestingly, the expression of RIP3, but not RIP1 or MLKL, was downregulated in MEFs bearing IDH1 R132Q (Figure 3A). Parallel results were obtained for three additional $IDH1^{WT/WT}$, three $IDH1^{WT/Mut}$, and two $IDH1^{Mut/Mut}$ MEF lines generated from an independent set of littermate embryos (Figure 3B). To confirm that IDH1 R132Q reduces RIP3 expression, we overexpressed IDH1 R132Q or IDH1 R132H in $IDH1^{WT/WT}$ MEFs and detected downregulation of RIP3 in cells expressing the IDH1 R132 mutants, but not WT IDH1 (Figure 3C). Moreover, treatment of $IDH1^{WT/WT}$ MEFs, or L929 and HT-29 cells, with exogenous 2-HG efficiently decreased RIP3 expression (Figure 3D). Thus, the 2-HG produced by IDH1 R132 mutant enzymes reduces intracellular RIP3 protein.

Because RIP3 is required for necroptosis, the low level of RIP3 in cells carrying an IDH1 mutation could be the cause of their resistance to TNF-α-induced necroptosis. To test this hypothesis, we overexpressed RIP3 in $IDH1^{Mut/Mut}$ MEFs to determine whether RIP3 could rescue the insensitivity of these cells to TNF-α-induced necroptosis and showed that this was indeed the case (Figure 3E). Collectively, these data demonstrate that the product of IDH1 R132 mutant enzymes can reduce intracellular RIP3 such that cells become resistant to TNF-α-induced necroptosis.

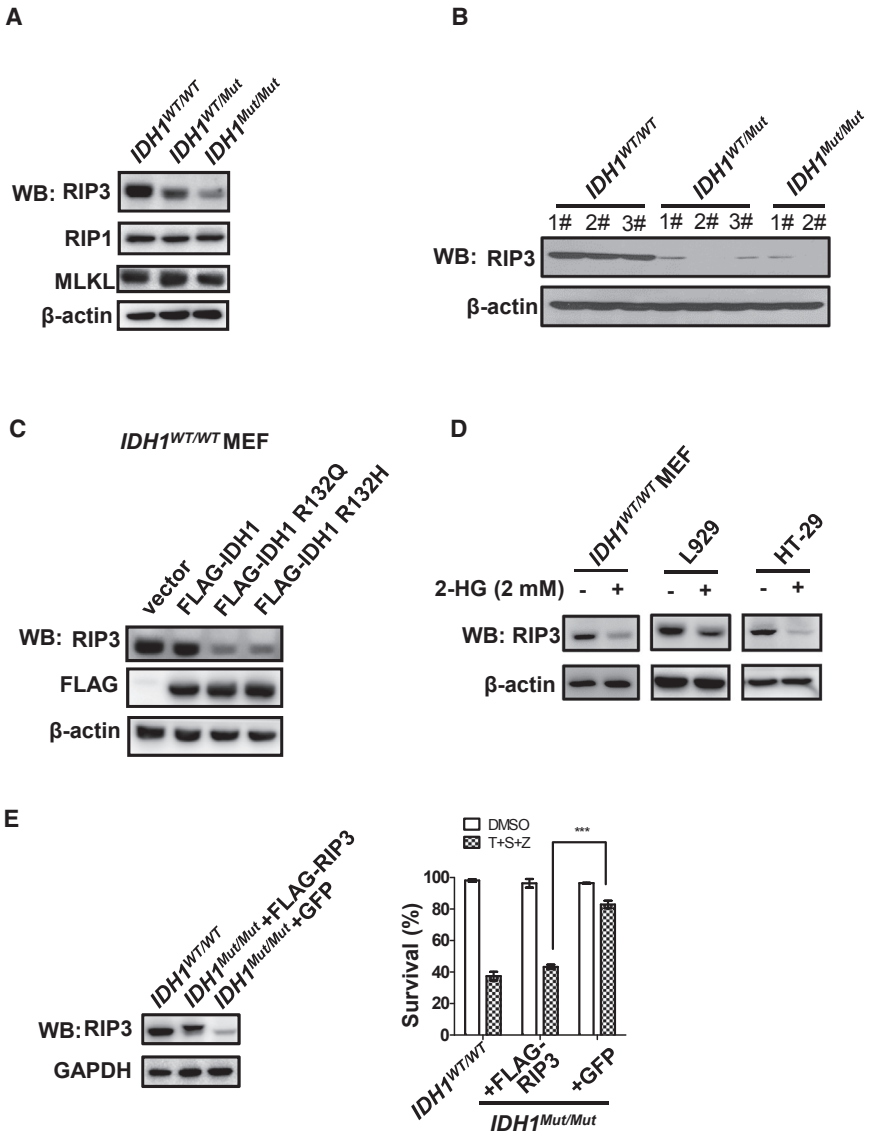

Figure 3. 2-HG Desensitizes Cells to TNF-α-Induced Necroptosis via Suppression of RIP3 Expression

(A) Western blot to detect the indicated proteins in untreated *IDH1*$^{WT/WT}$, *IDH1*$^{WT/Mut}$, and *IDH1*$^{Mut/Mut}$ MEFs.

(B) Western blot to detect RIP3 protein in three *IDH1*$^{WT/WT}$, three *IDH1*$^{WT/Mut}$, and two *IDH1*$^{Mut/Mut}$ additional MEF lines.

(C) Western blot to detect the indicated proteins in *IDH1*$^{WT/WT}$ MEFs that were infected with empty lentivirus (vector) or lentivirus expressing FLAG-tagged WT IDH1, IDH1-R132Q, or IDH1-R132H and cultured for 7 days.

(D) Western blot to detect the indicated proteins in *IDH1*$^{WT/WT}$ MEF, L929, and HT-29 cells that were left untreated (–) or treated with 2-HG (+) for 7 days.

(E) *IDH1*$^{Mut/Mut}$ MEFs were infected with lentivirus expressing Flag-RIP3 or GFP. At 96 hr post-infection, these cells, as well as *IDH1*$^{WT/WT}$ MEFs, were treated with DMSO or T + S + Z for 20 hr. Left: western blot to detect RIP3 in these cells is shown. Glyceraldehyde 3-phosphate dehydrogenase (GADPH), loading control. Right: survival of these cells determined by flow cytometric viability analysis as in Figure 1 is shown.

IDH1 R132 Mutation Promotes Hypermethylation of the RIP3 Promoter

To dissect the mechanism underlying the RIP3 downregulation mediated by IDH1 R132 mutation, we examined whether this downregulation occurs at the gene expression or protein stability level. Treatment of *IDH1*$^{Mut/Mut}$ and *IDH1*$^{WT/WT}$ MEFs with the proteasome inhibitor MG132, the calpain inhibitor ALLN, or the lysosome inhibitors NH_4Cl or chloroquine had no effect on RIP3 protein levels (Figure 4A), indicating that RIP3 protein degradation is unlikely to be the cause of the reduced RIP3 protein in IDH1-mutated cells. However, when we used qRT-PCR to compare *RIP3* mRNA levels in *IDH1*$^{Mut/Mut}$ and *IDH1*$^{WT/WT}$ MEFs, we observed that *IDH1*$^{Mut/Mut}$ MEFs had much less *RIP3* mRNA than *IDH1*$^{WT/WT}$ MEFs (Figure 4B). Thus, the downregulation of RIP3 expression induced by IDH1 mutation appears to occur at the transcriptional level.

Because 2-HG stimulates DNA hypermethylation (Sasaki et al., 2012b), and the methylation status of the *RIP3* promoter near its TSS controls its expression (Koo et al., 2015), we used bisulfite-sequencing PCR to determine whether 2-HG stimulates DNA hypermethylation in CpG islands near the RIP3 TSS. *IDH1*$^{Mut/Mut}$ MEFs exhibited much greater methylation of most CpG islands in this region than did *IDH1*$^{WT/WT}$ MEFs (Figures 4C and 4D). Moreover, 2-HG treatment of *IDH1*$^{WT/WT}$ MEFs increased *RIP3* CpG island methylation (Figures 4C and 4D). Thus, 2-HG produced by IDH1 R132Q stimulates hypermethylation near the *RIP3* TSS, which in turn leads to transcriptional silencing of RIP3.

DNMT1 Is Required for 2-HG-Mediated RIP3 Downregulation

As noted above, DNMT1, DNMT3a, and DNMT3b are the primary agents of DNA methylation in mammalian cells, whereas the TET proteins are essential for demethylation. DNA hypermethylation can result when high 2-HG levels block TET2 function. It has been previously shown that MEFs do not express TET1 or TET3 at all and show only very low levels of TET2 mRNA (Ito et al., 2010). Consistent with this result, we failed to detect TET2 protein in our MEF lines (Figure S1A). Nonetheless, when we treated *TET2* knockout (KO) MEFs with 2-HG, we observed efficient downregulation of RIP3 protein despite their lack of TET2 (Figure S1B). These results exclude a role for TET proteins

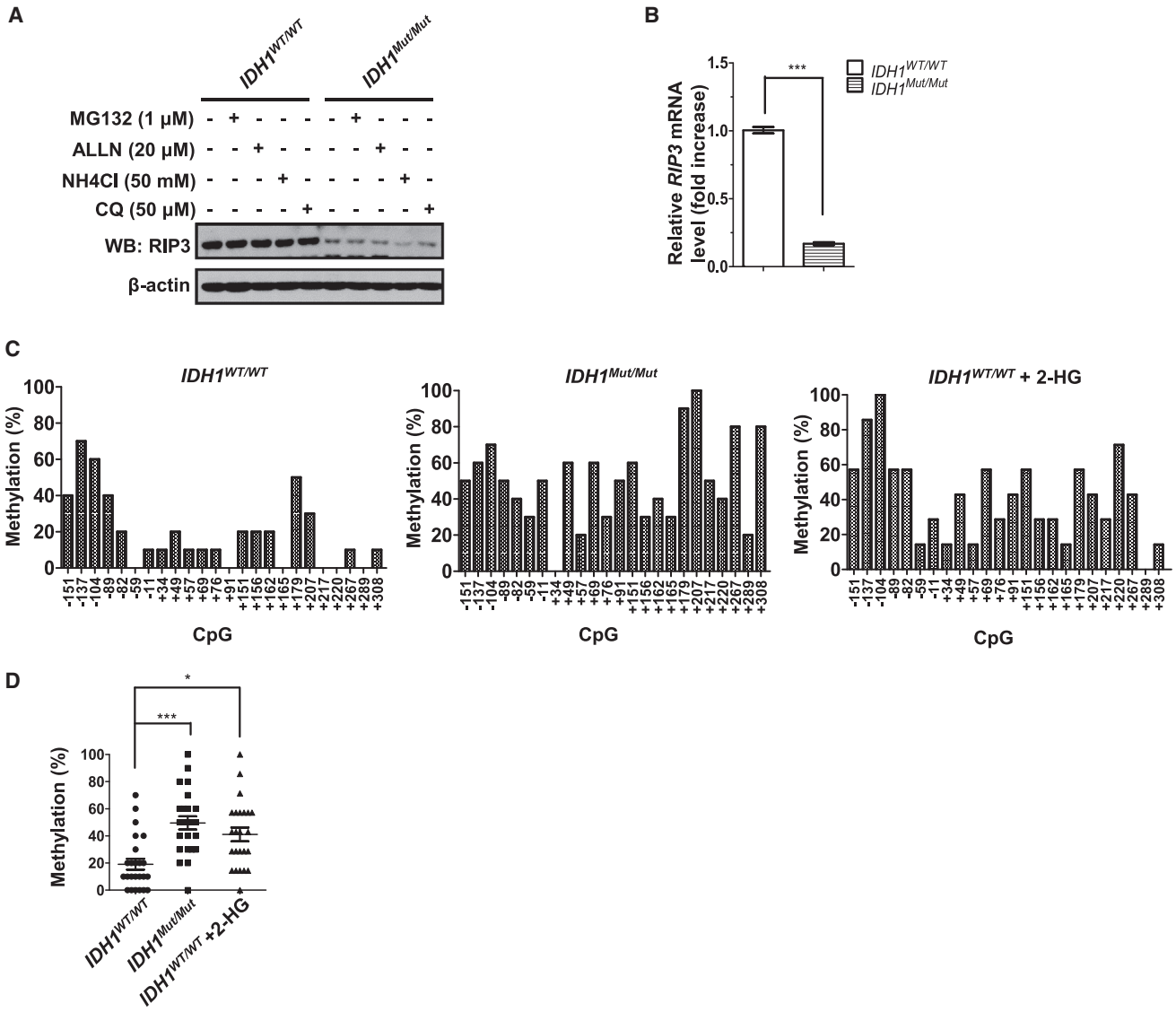

Figure 4. IDH1 R132 Mutation Induces Hypermethylation of the *RIP3* Promoter near the TSS

(A) Western blot to detect RIP3 in *IDH1*$^{WT/WT}$ and *IDH1*$^{Mut/Mut}$ MEFs that were left untreated (−) or treated (+) for 8 hr with the proteasome inhibitor MG132, the calpain inhibitor ALLN, or the lysosome inhibitors NH_4Cl or chloroquine, as indicated.

(B) qRT-PCR analysis of relative *RIP3* mRNA levels in *IDH1*$^{WT/WT}$ and *IDH1*$^{Mut/Mut}$ MEFs. Data were normalized to *GAPDH* mRNA and are presented relative to the level in *IDH1*$^{WT/WT}$ MEFs.

(C) Percent methylation levels of the indicated CpG islands in the *RIP3* promoter near the TSS (−151 to +309) in untreated *IDH1*$^{WT/WT}$ MEFs, untreated *IDH1*$^{Mut/Mut}$ MEFs, and 2-HG-treated *IDH1*$^{WT/WT}$ MEFs, as determined by bisulfite modification and DNA sequencing (see Experimental Procedures). The methylation percentage of each column was calculated from the DNA sequencing results of ten independent clones.

(D) Statistical analysis of differences in methylation levels of the CpG islands analyzed in (C). Each dot represents the mean methylation level of a single CpG island.

in the 2-HG-induced silencing of RIP3 in MEFs. Apart from this, published studies have demonstrated that 2-HG could regulate gene expression via impairing activity of some lysine-specific histone demethylases (KDMs) (Lu et al., 2012; Xu et al., 2011). We used short hairpin RNAs (shRNAs) to knock down KDM2A, KDM2B, or KDM4C expression and found that the reduction of KDM2A, KDM2B, or KDM4C expression did not affect RIP3 protein level in either *IDH1*$^{WT/WT}$ or *IDH1*$^{Mut/Mut}$ MEFs (Figures S1C–S1E), indicating that KDM2A, KDM2B, and KDM4C is not involved in transcriptional silencing of RIP3.

Next, we treated *IDH1*$^{WT/WT}$ and *IDH1*$^{Mut/Mut}$ MEFs with 5-aza-2′-deoxycytidine (5-AD), a well-known DNMT inhibitor, and found that this treatment restored RIP3 mRNA and protein expression level in *IDH1*$^{Mut/Mut}$ MEFs (Figures 5A and 5B). Similarly, 5-AD pretreatment of *IDH1*$^{WT/WT}$ MEFs abrogated 2-HG-induced RIP3 downregulation (Figure 5C). We then used shRNAs to knock

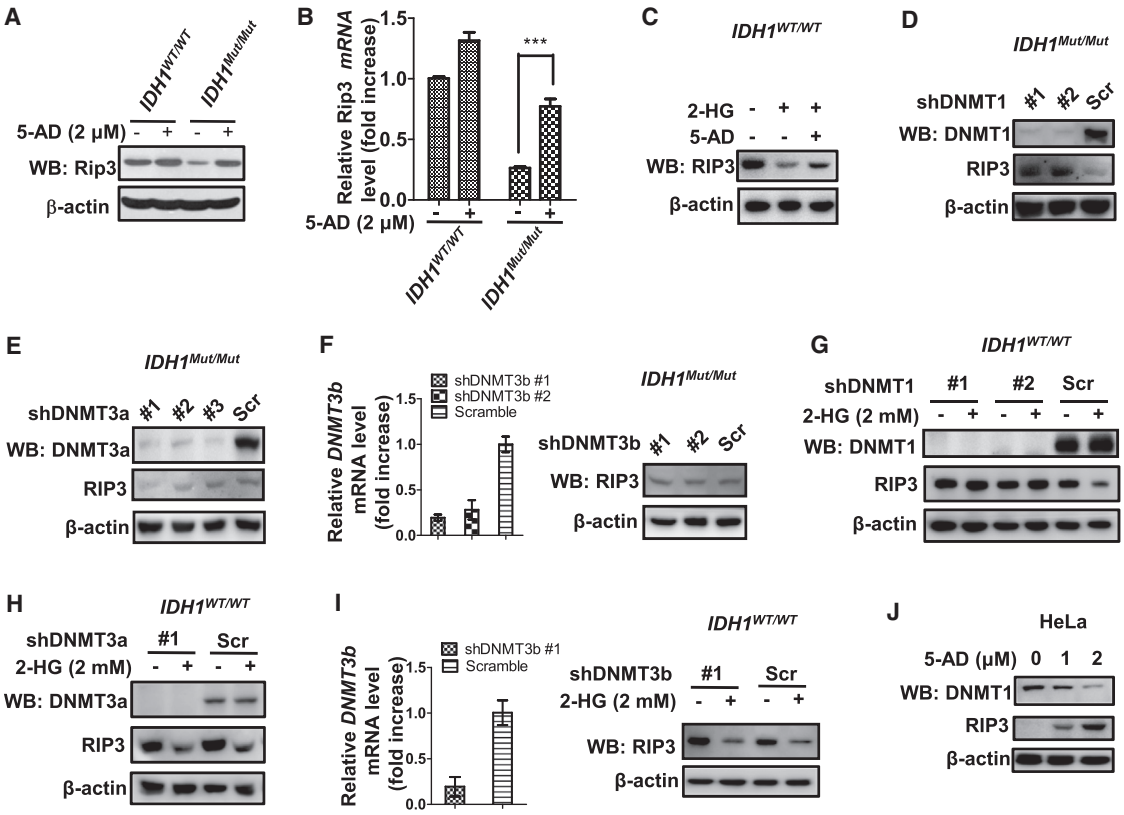

Figure 5. DNMT1 Is Required for 2-HG-Mediated Downregulation of RIP3

(A and B) *IDH1*$^{WT/WT}$ and *IDH1*$^{Mut/Mut}$ MEFs were left untreated (–) or treated with 5-AD (+) for 4 days. (A) Western blot to detect RIP3 in these cells is shown. (B) qRT-PCR analysis to determine relative *RIP3* mRNA levels in these cells is shown (as in Figure 4B).

(C) Western blot to detect RIP3 in *IDH1*$^{WT/WT}$ MEFs that were left untreated (–) or treated for 4 days (+) with DMSO, 2-HG (2 mM), or 2-HG (2 mM) + 5-AD (2 μM), as indicated.

(D) Western blot to detect the indicated proteins in *IDH1*$^{Mut/Mut}$ MEFs that were infected with lentiviruses expressing one of two independent *DNMT1* shRNAs (nos. 1 and 2), or scrambled control shRNA (Scr), for 96 hr.

(E) Western blot to detect the indicated proteins in *IDH1*$^{Mut/Mut}$ MEFs that were infected with lentiviruses expressing one of three independent *DNMT3a* shRNAs (nos. 1–3) or Scr for 96 hr.

(F) *IDH1*$^{Mut/Mut}$ MEFs were infected with lentiviruses expressing Scr or two independent *DNMT3b* shRNAs for 96 hr. Left: qRT-PCR analysis to determine relative *DNMT3b* mRNA levels in these cells is shown (as in Figure 4B). Right: western blot to detect RIP3 in these cells is shown.

(G) Western blot to detect the indicated proteins in *IDH1*$^{WT/WT}$ MEFs in which *DNMT1* was knocked down by infection with lentiviruses expressing one of two *DNMT1* shRNAs or Scr. Infected cells were then left untreated (–) or treated with 2-HG (+) for 7 days.

(H) Western blot to detect the indicated proteins in *IDH1*$^{WT/WT}$ MEFs in which *DNMT3a* was knocked down by infection with lentivirus expressing *DNMT1* shRNA or Scr. Infected cells were then left untreated (–) or treated with 2-HG (+) for 7 days.

(I) *DNMT3b* was knocked down in *IDH1*$^{WT/WT}$ MEFs by infection with lentivirus expressing *DNMT3b* shRNA or Scr. Infected cells were then left untreated (–) or treated with 2-HG (+) for 7 days. Left: qRT-PCR analysis to determine relative *DNMT3b* mRNA levels in these cells is shown (as in Figure 4B). Right: western blot to detect RIP3 in these cells is shown.

(J) Western blot to detect the indicated proteins in HeLa cells that were treated with indicated doses of 5-AD for 4 days.

down *DNMT1*, *DNMT3a*, or *DNMT3b* in *IDH1*$^{Mut/Mut}$ MEFs. Loss of *DNMT1* (Figure 5D), but not *DNMT3a* or *DNMT3b* (Figures 5E and 5F), restored RIP3 expression in the mutant cells. In *IDH1*$^{WT/WT}$ MEFs, knockdown of *DNMT1* (Figure 5G), but not *DNMT3a* (Figure 5H) or *DNMT3b* (Figure 5I), abolished the ability of 2-HG to decrease RIP3 expression. Finally, we examined the effect of 5-AD on DNMT1 expression by HeLa cells, which normally express high levels of DNMT but have undetectable RIP3. As expected, 5-AD treatment significantly increased RIP3 protein in HeLa cells (Figure 5J). All these results demonstrate that DNMT1 is critical for 2-HG-induced RIP3 downregulation.

2-HG Enhances the Association of DNMT1 with the RIP3 Promoter

We next explored how DNMT1 participated in 2-HG-induced RIP3 downregulation. First, we treated *IDH1*$^{WT/WT}$ MEFs with various doses of 2-HG but found that 2-HG failed to stimulate DNMT1 expression (Figure 6A). Next, we performed a drug affinity responsive target stability (DARTS) assay (Aghajan et al., 2010; Chin et al., 2014; Fu et al., 2015) to investigate whether 2-HG can bind directly to the DNMT1 protein. Since TET2 is known to interact with 2-HG (Xu et al., 2011), it was used as a positive control (Figure S2A). 2-HG protected DNMT1 from

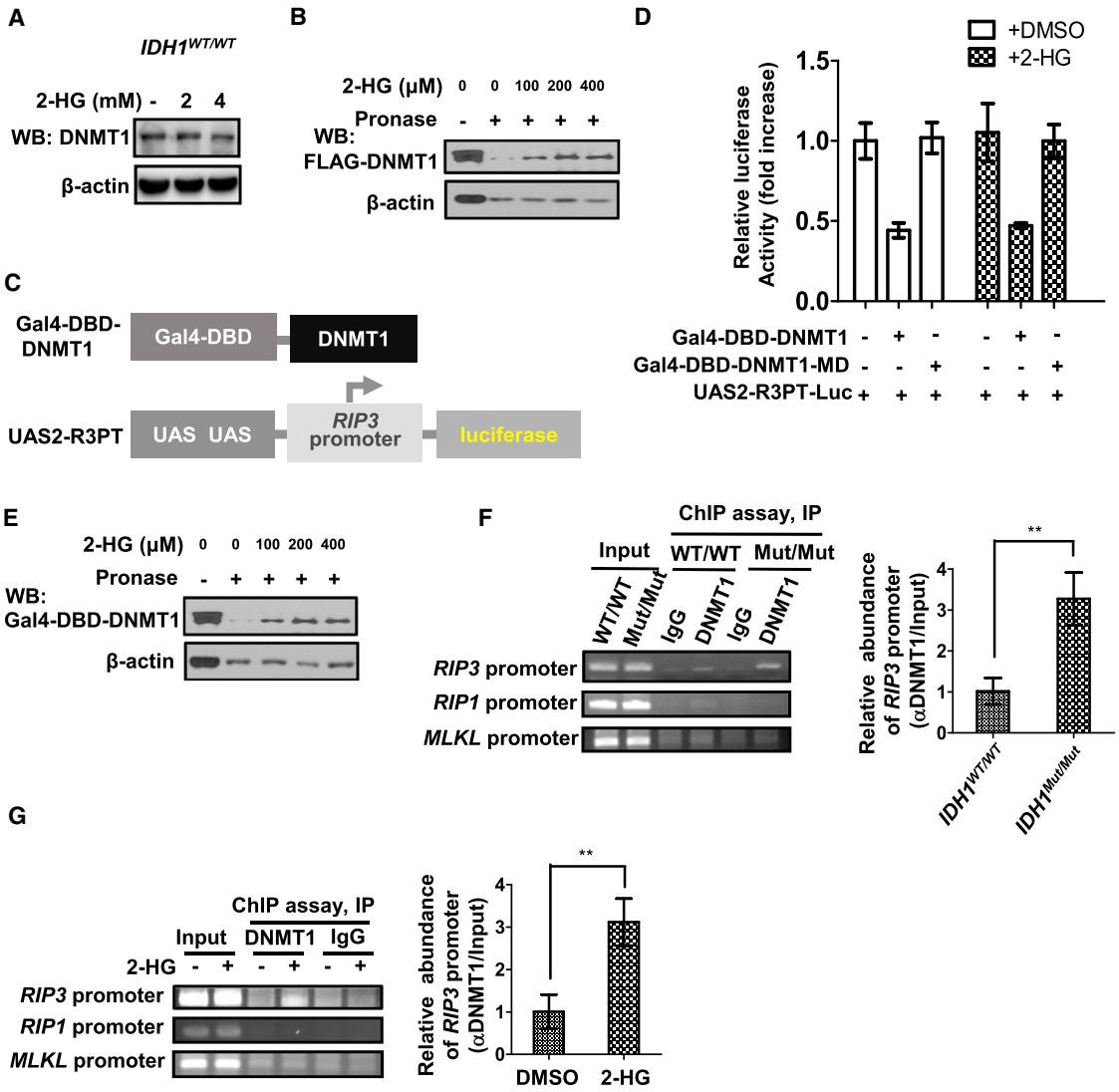

Figure 6. 2-HG Enhances the Association of DNMT1 with the *RIP3* Promoter Region

(A) Western blot to detect DNMT1 in *IDH1*$^{WT/WT}$ MEFs that were left untreated (−) or treated with the indicated doses of 2-HG for 7 days.

(B) Western blot of a drug affinity responsive target stability (DARTS) experiment identifying DNMT1 as a 2-HG-binding protein. HEK293T cells were transfected with FLAG-DNMT1 and incubated with the indicated doses of 2-HG for 1 hr on ice and 0.5 hr at room temperature, followed by Pronase digestion for 10 min.

(C) Schematic diagrams illustrating the fusion of DNMT1 to the Gal4-DNA-binding domain (DBD) and the fusion of luciferase (Luc) to duplicate upstream activation sequences (UASs) and the *RIP3* promoter (R3PT).

(D) Quantitation of relative luciferase activity in HEK293T cells that were transfected with the indicated combinations of the indicated plasmids, transferred to fresh culture medium at 8 hr post-transfection, and treated with DMSO or 2-HG (2 mM) for 36 hr.

(E) Western blot of a DARTS experiment demonstrating that 2-HG binds to DNMT1 in Gal4-DBD-DNMT-expressing HEK293T cells. The assay was performed as in (B).

(F) Left: chromatin immunoprecipitation (ChIP) assay performed using digested chromatin of untreated *IDH1*$^{WT/WT}$ and *IDH1*$^{Mut/Mut}$ MEFs and immunoglobulin G (IgG) (control) or anti-DNMT1 antibody (Ab). Purified DNA was analyzed by standard PCR using primers targeting the indicated promoter regions. Right: qRT-PCR analysis of the relative abundance of *RIP3* promoter segment in the ChIP assays in the left panel is shown. Results are expressed as the ratio of RIP3 promoter segment abundance after anti-DNMT1 IP versus input.

(G) Left: ChIP assay as in (F) of WT MEFs that were left untreated (−) or treated (+) with 2-HG (2 mM). Right: qRT-PCR analysis as in (F) of the relative abundance of RIP3 promoter segment in the cells in the left panel is shown.

Pronase-mediated digestion in a dose-dependent manner (Figure 6B), similar to that observed using TET2. To further study the interaction between 2-HG and DNMT1, we performed fluorescence quenching experiments. As shown in Figures S2B and S2C, the maximal fluorescence intensity of His-DNMT1 and a well-known 2-HG-binding protein PHD2, but not glutathione S-transferase (GST), was quenched by 2-HG in a dose-dependent manner. To map the binding site of 2-HG to

DNMT1, we constructed a series of DNMT1 truncations and performed additional fluorescence-quenching experiments. Among the five truncations (Figures S2D–S2H), 2-HG exclusively quenched the maximal fluorescence intensity of C-terminal region of DNMT1 protein (amino acids [aa] 1,121–1,617). Consistently, deletion of this region of DNMT1 totally abolished 2-HG-caused quenching (Figure S2I). Collectively, our data suggest that DNMT1 is a 2-HG-binding protein.

We then examined whether 2-HG induces hypermethylation of the *RIP3* TSS by stimulating DNMT1's methyltransferase activity or by enhancing the association of DNMT1 with the *RIP3* promoter. We used a reporter system in which DNMT1, or mutant DNMT1 lacking methyltransferase activity (DNMT1-MD) (aa 1–1,138), was fused to the Gal4-DNA-binding domain (DBD) (Robertson et al., 2000; Figure 6C). These fusion proteins (Gal4-DBD-DNMT1 and Gal4-DBD-DNMT1-MD) were separately co-expressed in HEK293T cells with a luciferase reporter containing two Gal4-binding sites (upstream activation sequence [UAS]) placed upstream of the mouse *RIP3* promoter (UAS2-R3PT-Luc). Gal4-DBD-DNMT1, but not Gal4-DBD-DNMT1-MD, strongly inhibited transcription from the *RIP3* promoter as measured by luciferase activity (Figure 6D). Importantly, although Gal4-DBD-DNMT1 retained its ability to associate with 2-HG, as indicated by DARTS assay (Figure 6E), its inhibitory effect on the *RIP3* promoter was not enhanced by 2-HG (Figure 6D), indicating that 2-HG does not stimulate the activity of DNMT1. This result was confirmed by in vitro assay showing that addition of 2-HG could not enhance enzyme activity of DNMT1 (Figure S2J). Next, we tested whether 2-HG enhanced the association of DNMT1 with the *RIP3* promoter region using chromatin immunoprecipitation (ChIP) assays. Indeed, many more DNA fragments derived from the *RIP3* promoter region, but not from the *RIP1* or *MLKL* promoter regions, co-precipitated with DNMT1 in $IDH1^{Mut/Mut}$ MEFs compared to $IDH1^{WT/WT}$ MEFs (Figure 6F). Similarly, treatment of $IDH1^{WT/WT}$ MEFs with 2-HG increased the affinity of binding between DNMT1 and the *RIP3* promoter (Figure 6G). Collectively, these data indicate that 2-HG enhances the association of DNMT1 with the *RIP3* promoter.

Downregulation of RIP3 by 2-HG Contributes to the Tumorigenic Functions of IDH1 R132 Mutant Enzymes

Because IDH1 mutations affect necroptosis, and necroptosis is likely a barrier to tumorigenesis, we speculated that the RIP3 downregulation induced by 2-HG might partially explain why IDH1 mutations are oncogenic. This hypothesis prompted us to investigate whether RIP3 was downregulated in human gliomas, which frequently harbor IDH1 R132H mutations (Balss et al., 2008; Watanabe et al., 2009; Yan et al., 2009). Western blotting confirmed that RIP3 protein was dramatically decreased in six human oligodendroglioma samples with IDH1 R132H mutation compared with five oligodendroglioma samples without IDH1 R132H mutation (Figure 7A), establishing a solid correlation between IDH1 R132H mutation and RIP3 downregulation. We next used cBioPortal (Cerami et al., 2012; Gao et al., 2013) to analyze gene expression patterns in samples of lower grade gliomas (283 patients) from The Cancer Genome Atlas (TCGA) database. Samples expressing mutant IDH1 R132 (219 patients) showed lower RIP3 mRNA levels than samples expressing WT IDH1 (64 patients; Figure 7B). These data indicate that IDH1 R132 mutations downregulate RIP3 expression in human brain cancers.

To systematically evaluate the in vivo effects of IDH1 R132Q mutation on tumorigenesis, we performed allograft tumor formation assays in nude mice. Necroptosis-resistant $IDH1^{Mut/Mut}$ MEFs transplanted into nude mice more potently induced tumor formation than did transplanted $IDH1^{WT/WT}$ MEFs (Figure 7C). Consistent with this result, inhibition of necroptosis by knockdown of *MLKL* promoted allograft tumor formation of $IDH1^{WT/WT}$ MEFs (Figure S3A). To demonstrate the role of IDH1 R132 mutation-mediated RIP3 downregulation in such tumorigenesis, we ectopically expressed RIP3 in $IDH1^{Mut/Mut}$ MEFs and performed the same assay. Ectopic expression of RIP3 diminished the ability of $IDH1^{Mut/Mut}$ MEFs to initiate tumor growth (Figure 7D). The effect of RIP3 was MLKL dependent (Figure S3B), confirming that necroptosis is responsible for RIP3-mediated inhibition of tumorigenesis driven by IDH1 mutations.

We conclude, based on the totality of our data, that the 2-HG produced by mutated IDH1 R132 enzymes enhances the binding of DNMT1 to the RIP3 promoter such that RIP3 is downregulated, inducing resistance to necroptosis, which contributes to the oncogenicity of the IDH1 mutation.

DISCUSSION

The fact that TET2 activity was blocked by the high levels of 2-HG produced by various tumors harboring IDH1/2 mutations (Figueroa et al., 2010; Turcan et al., 2012; Xu et al., 2011) led to the theory that TET2 inhibition was responsible for the DNA hypermethylation present in IDH1/2-mutated cells. However, our study establishes that 2-HG also regulates DNMT1 activity by promoting its binding to selected DNA regions, including the TSS of the *RIP3* promoter. Although DNMT1 is generally believed to be a maintenance methyltransferase, several reports have shown that it also has de novo DNA methylation activity (Fatemi et al., 2002; Pradhan et al., 1997; Rangel-Salazar et al., 2011). Our data support this contention because DNMT1 clearly hypermethylates the *RIP3* promoter in cells expressing IDH1 R132 mutant enzymes. This hypermethylation of the *RIP3* promoter downregulates RIP3 expression, which results in desensitization of the cell to TNF-α-induced necroptosis. This resistance to necroptosis may support the survival of incipient cancer cells, eventually leading to tumor formation.

2-HG is believed to competitively inhibit α-KG-dependent dioxygenases, including the TETs (Figueroa et al., 2010; Losman et al., 2013; Xu et al., 2011), and structural studies have indicated that 2-HG can bind to the α-KG-binding sites of these enzymes and block their activity (Xu et al., 2011). It has also been reported that DNMT1-dependent hypermethylation silences RIP3 expression in a variety of cancer cell lines (Koo et al., 2015). In our study, we found that 2-HG might bind directly to DNMT1 and increased its binding affinity for the *RIP3* promoter. We hypothesize that 2-HG binding to DNMT1 may induce a conformational change in the DNMT1 protein that favors its binding to selected DNA regions, but defining the mechanism by which 2-HG affects the function of DNMT1 awaits further investigation. Our present data show that 2-HG-dependent DNMT1 regulation operates not

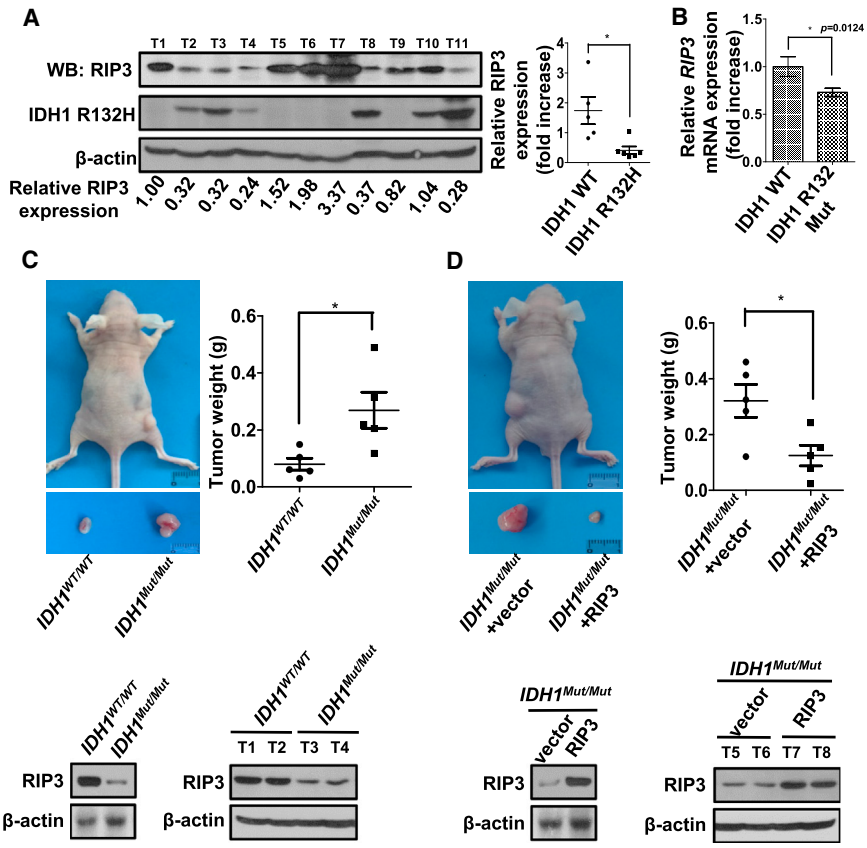

Figure 7. Downregulation of RIP3 by 2-HG Contributes to the Tumorigenicity of IDH1 R132 Mutant Enzymes

(A) Left: western blot to detect the indicated proteins in 11 clinical specimens (T1–11) of human oligodendrogliomas. Numbers indicating relative RIP3 protein levels appear below the blot and are expressed as the integrated density value (IDV) as determined by ImageJ software and after normalization to β-actin IDV. The relative RIP3 expression of tumor sample 1 (T1) was arbitrarily set to 1.00. Right: quantitation of relative RIP3 protein levels in tumor samples without IDH1 R132H mutation (T1, T5–T7, and T9) compared to those in tumors with IDH1 R132H mutation (T2–T4, T8, T10, and T11) is shown.

(B) Quantitation of relative RIP3 mRNA levels in 283 patient samples from the TCGA database as analyzed by using cBioPortal. Results are based on data generated by the TCGA Research Network: https://cancergenome.nih.gov/. Samples expressing WT IDH1 (64 patients) were compared with samples expressing IDH1 R132 mutants (219 patients).

(C) Primary *IDH1*$^{WT/WT}$ and *IDH1*$^{Mut/Mut}$ MEFs were transformed with Ras V12+E1A, and 2 × 10^6 cells were injected subcutaneously into contralateral flanks of nude mice (n = 5/group). Mice were sacrificed at 3 weeks post-injection. Upper left: representative tumors isolated from *IDH1*$^{WT/WT}$ or *IDH1*$^{Mut/Mut}$ allograft-bearing mice are shown. Upper right: quantitation of tumor weights is shown. Dots represent weights of individual tumors in five mice. Lower left: western blot to detect RIP3 in the indicated transformed MEF lines is shown. Lower right: western blot to detect RIP3 in two allograft tumors per group is shown.

(D) *IDH1*$^{Mut/Mut}$ MEFs were infected with empty lentivirus (vector) or lentivirus expressing RIP3. At 96 hr post-infection, infected cells were subjected to allograft tumor assays in nude mice and analyzed as in (C). Data are presented as mean ± SEM (A–D).

only in MEF but also in mouse L929 cells and human HT-29 cells, indicating that regulation of DNMT1 is a previously unidentified global function of 2-HG. Fluorescence-quenching experiments of DNMT1 truncations suggested that 2-HG bound DNMT1 at its C-terminal region (Figures S2D–S2I). We used PatchDock to predict the binding site of 2-HG to DNMT1 (aa 1,121–1,617), which showed that amino acids R1311, Q1340, and S1342 and R1493 and H1505 might be the potential binding pockets. But replacing these five amino acids with alanine (DNMT1-5 mutant [R1311A/Q1340A/S1342A/R1493A/H1505A]) had no effect on the affinity to 2-HG as compared with DNMT1–5 (Figures S4 and S2H). The 2-HG binding site in DNMT1 awaits further investigation.

The concept that apoptosis serves as a natural barrier to cancer development is currently well accepted, and resistance to cell death is regarded as a hallmark of cancer cells (Hanahan and Weinberg, 2011). Apoptosis is often triggered by stimuli delivered via interferons or by ligands for Toll-like receptors or death receptors (TNF-α and Fas), but these stimuli can also trigger necroptosis (He et al., 2011a; Holler et al., 2000; Zhang et al., 2009). RIP3 is a key component in the necroptosis pathway and is markedly downregulated in various tumor types, including leukemia, colon cancer, breast cancer, and lung cancer (Fukasawa et al., 2006; Koo et al., 2015; Liu et al., 2012; Moriwaki et al., 2015). In addition, SNPs in the genomic *RIP3* gene are closely associated with an increased risk of non-Hodgkin's lymphoma (Cerhan et al., 2007). These data suggest that necroptosis may function as an additional barrier against cancer development. If so, downregulation of RIP3 would compromise the response of tumor cells to necroptotic stimuli and could contribute to the initiation and development of various cancers. This theory is further supported by a recent study identifying RIP3 and the inflammasome as major tumor suppressors in AML (Höckendorf et al., 2016). We have shown that RIP3 expression is downregulated in cells expressing mutant IDH1 R132 due to hypermethylation of the *RIP3* promoter and that these cells become desensitized to necroptosis. We also demonstrated that RIP3 downregulation facilitated the growth of allograft tumors in nude mice, further indicating that RIP3 is a vital tumor suppressor. However, how necroptosis is induced in tumor cells in vivo is a question remaining to be answered. RIP3-dependent necroptosis can occur in a number of situations that are independent of TNF-α. Spontaneous necroptosis can occur when suppression factors, such as phosphatase Ppm1b (Chen et al., 2015), RIP1, FADD, or caspase-8, were impaired. Because RIP3 has a tendency to auto-phosphorylate, we speculate that any alternation on the suppression mechanisms of RIP3 auto-phosphorylation in vivo would promote RIP3-dependent

necroptosis. Further investigation is needed to find out the detailed mechanism of how necroptosis is engaged in inhibiting tumor growth in vivo. Collectively, our research sheds light on the mechanisms underlying the tumorigenesis driven by mutated IDH1 enzymes producing high levels of 2-HG.

Accumulating evidence has established that various chemotherapeutic drugs can induce the necroptosis of cancer cells that cannot undergo apoptosis. For example, cisplatin can induce the RIP3-dependent necroptosis of apoptosis-resistant esophageal cancer cells (Xu et al., 2014). Similarly, *RIP3* knockdown in HT-29 cells inhibits cell death induced by doxorubicin and etoposide, whereas ectopic RIP3 expression in HeLa, MDAMB231, and Huh-7 cells (which lack endogenous RIP3 expression) heightens sensitivity to both etoposide and doxorubicin (Koo et al., 2015). Taken together, these data suggest that RIP3 is essential for necroptosis triggered by anticancer agents. Because RIP3 is frequently silenced by hypermethylation in cancer cells, the use of hypomethylating agents, such as 5-AD, can successfully restore RIP3 expression in a variety of cell types, sensitizing them to necroptosis induced by chemotherapeutic agents (Koo et al., 2015). Based on our study, we propose that combining hypomethylating agents with common chemotherapeutic agents could be an effective treatment for any cancer whose initiation and development is driven by IDH1/2 mutation.

EXPERIMENTAL PROCEDURES

Cell Lines, Reagents, Antibodies, and Constructs

Detailed information on cell lines, reagents, antibodies, and constructs is described in Supplemental Experimental Procedures.

Cell Viability

The viabilities of MEFs, HT29, and L929 cells were determined by propidium iodide (PI) exclusion. Briefly, trypsinized cells were collected by centrifugation, washed once with PBS, and resuspended in PBS containing 5 μg/mL PI (Sigma; P4170). PI incorporation was quantified on a BD Calibur FACScan flow cytometer.

2-HG Measurement by LC-MS

LC-MS analysis of 2-HG levels was performed as described (Dang et al., 2009). Details appear in Supplemental Experimental Procedures.

DNA Methylation

Cellular genomic DNA was isolated and purified by Proteinase K digestion and phenol chloroform extraction. Purified genomes were modified with bisulfate and harvested using the CpGenome Turbo Bisulfite Modification Kit (Millipore; S7847) according to the manufacturer's instructions. The modified *RIP3* promoter region near the TSS was amplified with the following primers: F: 5′-AGAGAATTCGGATCCTGGAGTTAAGGGGTTTAAGAGAGAT-3′ and R: 5′-CTTCCATGGCTCGAGCTTTATCCCCTACCTCAAAAAAAAC-3′. The PCR product of each reaction was cloned into pBKS, and ten clones were randomly picked for sequencing. The methylation level of each site was expressed as the mean percentage of the site that was methylated according to sequencing data obtained from ten clones.

ChIP

ChIP assays were performed following the standard protocol of SimpleChIP Enzymatic Chromation IP Kit (Cell Signaling Technology; no. 9002). Details appear in Supplemental Experimental Procedures.

Animal Experiments and Patient Samples

All animal experimental protocols were approved by the Institutional Animal Care and Use Committee at Xiamen University. Glioma samples were obtained with approval of the research ethics boards of Xiamen University and Huanhu Hospital. Written informed consent was obtained from all patients. For detailed sample information, please refer to Supplemental Experimental Procedures.

DARTS Assays

DARTS was performed as described (Lomenick et al., 2009) with minor modifications. Details appear in Supplemental Experimental Procedures.

Statistics

Two-tailed Student's t test was used to compare differences between treated and control groups. Differences with p values < 0.05 were considered statistically significant: *p < 0.05; **p < 0.01; ***p < 0.001.

SUPPLEMENTAL INFORMATION

Supplemental Information includes Supplemental Experimental Procedures and four figures and can be found with this article online at http://dx.doi.org/10.1016/j.celrep.2017.05.012.

AUTHOR CONTRIBUTIONS

Z.Y., B.J., Y.W., Q.L., and J.H. conceived and designed experiments. Z.Y., B.J., Y.W., H.N., J.Z., J.X., and J.R. performed experiments. M.S. performed surgical excisions and prepared primary human glioma samples. Z.Y., B.J., Q.L., and J.H. interpreted the data and wrote the original manuscript. Q.L., J.H., L.-M.H., and T.W.M. provided helpful discussions and refined the paper.

ACKNOWLEDGMENTS

This work was supported by the National Basic Research Program of China (973 Program; 2015CB553800, 2013CB944903, and 2014CB541804), the National Natural Science Foundation of China (91029304, 31420103910, 31330047, 81630042, 81372702, 81402285, and 31571473), the 111 Project (B12001), the Fundamental Research Funds for the Central Universities (20720140552 and 10120100002), and the National Science Foundation of China for Fostering Talents in Basic Research (grant no. J1310027). We thank Drs. Jie-Kai Chen and Duanqing Pei (Guangzhou Institutes of Biomedicine and Health, Chinese Academy of Sciences) for providing *TET2* KO MEFs. We also thank Drs. Rob A. Cairns and Satoshi Inoue (The Campbell Family Institute for Breast Cancer Research, University Health Network) for important comments and Dr. Mary Saunders for scientific editing of the manuscript.

Received: November 18, 2016
Revised: March 31, 2017
Accepted: May 2, 2017
Published: May 30, 2017

REFERENCES

Abbas, S., Lugthart, S., Kavelaars, F.G., Schelen, A., Koenders, J.E., Zeilemaker, A., van Putten, W.J., Rijneveld, A.W., Löwenberg, B., and Valk, P.J. (2010). Acquired mutations in the genes encoding IDH1 and IDH2 both are recurrent aberrations in acute myeloid leukemia: prevalence and prognostic value. Blood *116*, 2122–2126.

Aghajan, M., Jonai, N., Flick, K., Fu, F., Luo, M., Cai, X., Ouni, I., Pierce, N., Tang, X., Lomenick, B., et al. (2010). Chemical genetics screen for enhancers of rapamycin identifies a specific inhibitor of an SCF family E3 ubiquitin ligase. Nat. Biotechnol. *28*, 738–742.

Amary, M.F., Bacsi, K., Maggiani, F., Damato, S., Halai, D., Berisha, F., Pollock, R., O'Donnell, P., Grigoriadis, A., Diss, T., et al. (2011). IDH1 and IDH2 mutations are frequent events in central chondrosarcoma and central and periosteal chondromas but not in other mesenchymal tumours. J. Pathol. *224*, 334–343.

Balss, J., Meyer, J., Mueller, W., Korshunov, A., Hartmann, C., and von Deimling, A. (2008). Analysis of the IDH1 codon 132 mutation in brain tumors. Acta Neuropathol. *116*, 597–602.

Bird, A.P., and Wolffe, A.P. (1999). Methylation-induced repression–belts, braces, and chromatin. Cell *99*, 451–454.

Bleeker, F.E., Lamba, S., Leenstra, S., Troost, D., Hulsebos, T., Vandertop, W.P., Frattini, M., Molinari, F., Knowles, M., Cerrato, A., et al. (2009). IDH1 mutations at residue p.R132 (IDH1(R132)) occur frequently in high-grade gliomas but not in other solid tumors. Hum. Mutat. *30*, 7–11.

Borger, D.R., Tanabe, K.K., Fan, K.C., Lopez, H.U., Fantin, V.R., Straley, K.S., Schenkein, D.P., Hezel, A.F., Ancukiewicz, M., Liebman, H.M., et al. (2012). Frequent mutation of isocitrate dehydrogenase (IDH)1 and IDH2 in cholangiocarcinoma identified through broad-based tumor genotyping. Oncologist *17*, 72–79.

Cerami, E., Gao, J., Dogrusoz, U., Gross, B.E., Sumer, S.O., Aksoy, B.A., Jacobsen, A., Byrne, C.J., Heuer, M.L., Larsson, E., et al. (2012). The cBio cancer genomics portal: an open platform for exploring multidimensional cancer genomics data. Cancer Discov. *2*, 401–404.

Cerhan, J.R., Ansell, S.M., Fredericksen, Z.S., Kay, N.E., Liebow, M., Call, T.G., Dogan, A., Cunningham, J.M., Wang, A.H., Liu-Mares, W., et al. (2007). Genetic variation in 1253 immune and inflammation genes and risk of non-Hodgkin lymphoma. Blood *110*, 4455–4463.

Chen, W., Wu, J., Li, L., Zhang, Z., Ren, J., Liang, Y., Chen, F., Yang, C., Zhou, Z., Su, S.S., et al. (2015). Ppm1b negatively regulates necroptosis through dephosphorylating Rip3. Nat. Cell Biol. *17*, 434–444.

Chen, D., Yu, J., and Zhang, L. (2016). Necroptosis: an alternative cell death program defending against cancer. Biochim. Biophys. Acta *1865*, 228–236.

Chin, R.M., Fu, X., Pai, M.Y., Vergnes, L., Hwang, H., Deng, G., Diep, S., Lomenick, B., Meli, V.S., Monsalve, G.C., et al. (2014). The metabolite α-ketoglutarate extends lifespan by inhibiting ATP synthase and TOR. Nature *510*, 397–401.

Dang, L., White, D.W., Gross, S., Bennett, B.D., Bittinger, M.A., Driggers, E.M., Fantin, V.R., Jang, H.G., Jin, S., Keenan, M.C., et al. (2009). Cancer-associated IDH1 mutations produce 2-hydroxyglutarate. Nature *462*, 739–744.

De Carli, E., Wang, X., and Puget, S. (2009). IDH1 and IDH2 mutations in gliomas. N. Engl. J. Med. *360*, 2248.

Ducray, F., Marie, Y., and Sanson, M. (2009). IDH1 and IDH2 mutations in gliomas. N. Engl. J. Med. *360*, 2248–2249.

Fatemi, M., Hermann, A., Gowher, H., and Jeltsch, A. (2002). Dnmt3a and Dnmt1 functionally cooperate during de novo methylation of DNA. Eur. J. Biochem. *269*, 4981–4984.

Figueroa, M.E., Abdel-Wahab, O., Lu, C., Ward, P.S., Patel, J., Shih, A., Li, Y., Bhagwat, N., Vasanthakumar, A., Fernandez, H.F., et al. (2010). Leukemic IDH1 and IDH2 mutations result in a hypermethylation phenotype, disrupt TET2 function, and impair hematopoietic differentiation. Cancer Cell *18*, 553–567.

Fu, X., Chin, R.M., Vergnes, L., Hwang, H., Deng, G., Xing, Y., Pai, M.Y., Li, S., Ta, L., Fazlollahi, F., et al. (2015). 2-hydroxyglutarate inhibits ATP synthase and mTOR signaling. Cell Metab. *22*, 508–515.

Fukasawa, M., Kimura, M., Morita, S., Matsubara, K., Yamanaka, S., Endo, C., Sakurada, A., Sato, M., Kondo, T., Horii, A., et al. (2006). Microarray analysis of promoter methylation in lung cancers. J. Hum. Genet. *51*, 368–374.

Gaal, J., Burnichon, N., Korpershoek, E., Roncelin, I., Bertherat, J., Plouin, P.F., de Krijger, R.R., Gimenez-Roqueplo, A.P., and Dinjens, W.N. (2010). Isocitrate dehydrogenase mutations are rare in pheochromocytomas and paragangliomas. J. Clin. Endocrinol. Metab. *95*, 1274–1278.

Gao, J., Aksoy, B.A., Dogrusoz, U., Dresdner, G., Gross, B., Sumer, S.O., Sun, Y., Jacobsen, A., Sinha, R., Larsson, E., et al. (2013). Integrative analysis of complex cancer genomics and clinical profiles using the cBioPortal. Sci. Signal. *6*, pl1.

Hanahan, D., and Weinberg, R.A. (2011). Hallmarks of cancer: the next generation. Cell *144*, 646–674.

Haselbeck, R.J., and McAlister-Henn, L. (1993). Function and expression of yeast mitochondrial NAD- and NADP-specific isocitrate dehydrogenases. J. Biol. Chem. *268*, 12116–12122.

He, S., Liang, Y., Shao, F., and Wang, X. (2011a). Toll-like receptors activate programmed necrosis in macrophages through a receptor-interacting kinase-3-mediated pathway. Proc. Natl. Acad. Sci. USA *108*, 20054–20059.

He, Y.F., Li, B.Z., Li, Z., Liu, P., Wang, Y., Tang, Q., Ding, J., Jia, Y., Chen, Z., Li, L., et al. (2011b). Tet-mediated formation of 5-carboxylcytosine and its excision by TDG in mammalian DNA. Science *333*, 1303–1307.

Höckendorf, U., Yabal, M., Herold, T., Munkhbaatar, E., Rott, S., Jilg, S., Kauschinger, J., Magnani, G., Reisinger, F., Heuser, M., et al. (2016). RIPK3 restricts myeloid leukemogenesis by promoting cell death and differentiation of leukemia initiating cells. Cancer Cell *30*, 75–91.

Holler, N., Zaru, R., Micheau, O., Thome, M., Attinger, A., Valitutti, S., Bodmer, J.L., Schneider, P., Seed, B., and Tschopp, J. (2000). Fas triggers an alternative, caspase-8-independent cell death pathway using the kinase RIP as effector molecule. Nat. Immunol. *1*, 489–495.

Inoue, S., Li, W.Y., Tseng, A., Beerman, I., Elia, A.J., Bendall, S.C., Lemonnier, F., Kron, K.J., Cescon, D.W., Hao, Z., et al. (2016). Mutant IDH1 downregulates ATM and alters DNA repair and sensitivity to DNA damage independent of TET2. Cancer Cell *30*, 337–348.

Ito, S., D'Alessio, A.C., Taranova, O.V., Hong, K., Sowers, L.C., and Zhang, Y. (2010). Role of Tet proteins in 5mC to 5hmC conversion, ES-cell self-renewal and inner cell mass specification. Nature *466*, 1129–1133.

Ito, S., Shen, L., Dai, Q., Wu, S.C., Collins, L.B., Swenberg, J.A., He, C., and Zhang, Y. (2011). Tet proteins can convert 5-methylcytosine to 5-formylcytosine and 5-carboxylcytosine. Science *333*, 1300–1303.

Kang, M.R., Kim, M.S., Oh, J.E., Kim, Y.R., Song, S.Y., Seo, S.I., Lee, J.Y., Yoo, N.J., and Lee, S.H. (2009). Mutational analysis of IDH1 codon 132 in glioblastomas and other common cancers. Int. J. Cancer *125*, 353–355.

Koo, G.B., Morgan, M.J., Lee, D.G., Kim, W.J., Yoon, J.H., Koo, J.S., Kim, S.I., Kim, S.J., Son, M.K., Hong, S.S., et al. (2015). Methylation-dependent loss of RIP3 expression in cancer represses programmed necrosis in response to chemotherapeutics. Cell Res. *25*, 707–725.

Li, E. (2002). Chromatin modification and epigenetic reprogramming in mammalian development. Nat. Rev. Genet. *3*, 662–673.

Liu, P., Xu, B., Shen, W., Zhu, H., Wu, W., Fu, Y., Chen, H., Dong, H., Zhu, Y., Miao, K., et al. (2012). Dysregulation of TNFα-induced necroptotic signaling in chronic lymphocytic leukemia: suppression of CYLD gene by LEF1. Leukemia *26*, 1293–1300.

Lomenick, B., Hao, R., Jonai, N., Chin, R.M., Aghajan, M., Warburton, S., Wang, J., Wu, R.P., Gomez, F., Loo, J.A., et al. (2009). Target identification using drug affinity responsive target stability (DARTS). Proc. Natl. Acad. Sci. USA *106*, 21984–21989.

Losman, J.A., Looper, R.E., Koivunen, P., Lee, S., Schneider, R.K., McMahon, C., Cowley, G.S., Root, D.E., Ebert, B.L., and Kaelin, W.G., Jr. (2013). (R)-2-hydroxyglutarate is sufficient to promote leukemogenesis and its effects are reversible. Science *339*, 1621–1625.

Lu, C., Ward, P.S., Kapoor, G.S., Rohle, D., Turcan, S., Abdel-Wahab, O., Edwards, C.R., Khanin, R., Figueroa, M.E., Melnick, A., et al. (2012). IDH mutation impairs histone demethylation and results in a block to cell differentiation. Nature *483*, 474–478.

Mardis, E.R., Ding, L., Dooling, D.J., Larson, D.E., McLellan, M.D., Chen, K., Koboldt, D.C., Fulton, R.S., Delehaunty, K.D., McGrath, S.D., et al. (2009). Recurring mutations found by sequencing an acute myeloid leukemia genome. N. Engl. J. Med. *361*, 1058–1066.

Moriwaki, K., Bertin, J., Gough, P.J., Orlowski, G.M., and Chan, F.K. (2015). Differential roles of RIPK1 and RIPK3 in TNF-induced necroptosis and chemotherapeutic agent-induced cell death. Cell Death Dis. *6*, e1636.

Noushmehr, H., Weisenberger, D.J., Diefes, K., Phillips, H.S., Pujara, K., Berman, B.P., Pan, F., Pelloski, C.E., Sulman, E.P., Bhat, K.P., et al.; Cancer Genome Atlas Research Network (2010). Identification of a CpG island methylator phenotype that defines a distinct subgroup of glioma. Cancer Cell *17*, 510–522.

Pansuriya, T.C., van Eijk, R., d'Adamo, P., van Ruler, M.A., Kuijjer, M.L., Oosting, J., Cleton-Jansen, A.M., van Oosterwijk, J.G., Verbeke, S.L., Meijer,

D., et al. (2011). Somatic mosaic IDH1 and IDH2 mutations are associated with enchondroma and spindle cell hemangioma in Ollier disease and Maffucci syndrome. Nat. Genet. *43*, 1256–1261.

Parsons, D.W., Jones, S., Zhang, X., Lin, J.C., Leary, R.J., Angenendt, P., Mankoo, P., Carter, H., Siu, I.M., Gallia, G.L., et al. (2008). An integrated genomic analysis of human glioblastoma multiforme. Science *321*, 1807–1812.

Pradhan, S., Talbot, D., Sha, M., Benner, J., Hornstra, L., Li, E., Jaenisch, R., and Roberts, R.J. (1997). Baculovirus-mediated expression and characterization of the full-length murine DNA methyltransferase. Nucleic Acids Res. *25*, 4666–4673.

Rangel-Salazar, R., Wickström-Lindholm, M., Aguilar-Salinas, C.A., Alvarado-Caudillo, Y., Døssing, K.B., Esteller, M., Labourier, E., Lund, G., Nielsen, F.C., Rodríguez-Ríos, D., et al. (2011). Human native lipoprotein-induced de novo DNA methylation is associated with repression of inflammatory genes in THP-1 macrophages. BMC Genomics *12*, 582.

Reik, W., Dean, W., and Walter, J. (2001). Epigenetic reprogramming in mammalian development. Science *293*, 1089–1093.

Robertson, K.D., Ait-Si-Ali, S., Yokochi, T., Wade, P.A., Jones, P.L., and Wolffe, A.P. (2000). DNMT1 forms a complex with Rb, E2F1 and HDAC1 and represses transcription from E2F-responsive promoters. Nat. Genet. *25*, 338–342.

Sasaki, M., Knobbe, C.B., Itsumi, M., Elia, A.J., Harris, I.S., Chio, I.I., Cairns, R.A., McCracken, S., Wakeham, A., Haight, J., et al. (2012a). D-2-hydroxyglutarate produced by mutant IDH1 perturbs collagen maturation and basement membrane function. Genes Dev. *26*, 2038–2049.

Sasaki, M., Knobbe, C.B., Munger, J.C., Lind, E.F., Brenner, D., Brüstle, A., Harris, I.S., Holmes, R., Wakeham, A., Haight, J., et al. (2012b). IDH1(R132H) mutation increases murine haematopoietic progenitors and alters epigenetics. Nature *488*, 656–659.

Sequist, L.V., Heist, R.S., Shaw, A.T., Fidias, P., Rosovsky, R., Temel, J.S., Lennes, I.T., Digumarthy, S., Waltman, B.A., Bast, E., et al. (2011). Implementing multiplexed genotyping of non-small-cell lung cancers into routine clinical practice. Ann. Oncol. *22*, 2616–2624.

Sjöblom, T., Jones, S., Wood, L.D., Parsons, D.W., Lin, J., Barber, T.D., Mandelker, D., Leary, R.J., Ptak, J., Silliman, N., et al. (2006). The consensus coding sequences of human breast and colorectal cancers. Science *314*, 268–274.

Tahiliani, M., Koh, K.P., Shen, Y., Pastor, W.A., Bandukwala, H., Brudno, Y., Agarwal, S., Iyer, L.M., Liu, D.R., Aravind, L., and Rao, A. (2009). Conversion of 5-methylcytosine to 5-hydroxymethylcytosine in mammalian DNA by MLL partner TET1. Science *324*, 930–935.

Turcan, S., Rohle, D., Goenka, A., Walsh, L.A., Fang, F., Yilmaz, E., Campos, C., Fabius, A.W., Lu, C., Ward, P.S., et al. (2012). IDH1 mutation is sufficient to establish the glioma hypermethylator phenotype. Nature *483*, 479–483.

Wang, L., Du, F., and Wang, X. (2008). TNF-alpha induces two distinct caspase-8 activation pathways. Cell *133*, 693–703.

Ward, P.S., Patel, J., Wise, D.R., Abdel-Wahab, O., Bennett, B.D., Coller, H.A., Cross, J.R., Fantin, V.R., Hedvat, C.V., Perl, A.E., et al. (2010). The common feature of leukemia-associated IDH1 and IDH2 mutations is a neomorphic enzyme activity converting alpha-ketoglutarate to 2-hydroxyglutarate. Cancer Cell *17*, 225–234.

Watanabe, T., Nobusawa, S., Kleihues, P., and Ohgaki, H. (2009). IDH1 mutations are early events in the development of astrocytomas and oligodendrogliomas. Am. J. Pathol. *174*, 1149–1153.

Xu, W., Yang, H., Liu, Y., Yang, Y., Wang, P., Kim, S.H., Ito, S., Yang, C., Wang, P., Xiao, M.T., et al. (2011). Oncometabolite 2-hydroxyglutarate is a competitive inhibitor of α-ketoglutarate-dependent dioxygenases. Cancer Cell *19*, 17–30.

Xu, Y., Lin, Z., Zhao, N., Zhou, L., Liu, F., Cichacz, Z., Zhang, L., Zhan, Q., and Zhao, X. (2014). Receptor interactive protein kinase 3 promotes Cisplatin-triggered necrosis in apoptosis-resistant esophageal squamous cell carcinoma cells. PLoS ONE *9*, e100127.

Yan, H., Parsons, D.W., Jin, G., McLendon, R., Rasheed, B.A., Yuan, W., Kos, I., Batinic-Haberle, I., Jones, S., Riggins, G.J., et al. (2009). IDH1 and IDH2 mutations in gliomas. N. Engl. J. Med. *360*, 765–773.

Zhang, D.W., Shao, J., Lin, J., Zhang, N., Lu, B.J., Lin, S.C., Dong, M.Q., and Han, J. (2009). RIP3, an energy metabolism regulator that switches TNF-induced cell death from apoptosis to necrosis. Science *325*, 332–336.

Zhang, D.W., Zheng, M., Zhao, J., Li, Y.Y., Huang, Z., Li, Z., and Han, J. (2011). Multiple death pathways in TNF-treated fibroblasts: RIP3- and RIP1-dependent and independent routes. Cell Res. *21*, 368–371.

Zhao, S., Lin, Y., Xu, W., Jiang, W., Zha, Z., Wang, P., Yu, W., Li, Z., Gong, L., Peng, Y., et al. (2009). Glioma-derived mutations in IDH1 dominantly inhibit IDH1 catalytic activity and induce HIF-1alpha. Science *324*, 261–265.